Monthly Notices
of the
ROYAL ASTRONOMICAL SOCIETY

MNRAS **449,** 88–93 (2015) doi:10.1093/mnras/stv279

3D MHD simulation of polarized emission in SN 1006

E. M. Schneiter,[1,2,3★] P. F. Velázquez,[4] E. M. Reynoso,[5,6] A. Esquivel[4] and F. De Colle[4]

[1]*Instituto de Astronomía Teórica y Experimental, Universidad Nacional de Córdoba, X5000BGR, Córdoba, Argentina*
[2]*Departamento de Materiales y Tecnologia, UNC, X5000JKP, Córdoba, Argentina*
[3]*Deparment of Astronomy & Oskar Klein Centre, Albanova, Stockholm University, SE-106 91 Stockholm, Sweden*
[4]*Instituto de Ciencias Nucleares, Universidad Nacional de Mexico, 04510, Mexico D. F. Mexico*
[5]*Instituto de Astronomía y Física del Espacio, Suc. 28, CP: 1428 Buenos Aires, Argentina*
[6]*Physics Department, Faculty of Exact and Natural Sciences, University of Buenos Aires, C1428EHA, Argentina*

Accepted 2015 February 9. Received 2015 February 9; in original form 2014 December 17

ABSTRACT

We use three-dimensional magnetohydrodynamic simulations to model the supernova remnant SN 1006. From our numerical results, we have carried out a polarization study, obtaining synthetic maps of the polarized intensity, the Stokes parameter Q, and the polar-referenced angle, which can be compared with observational results. Synthetic maps were computed considering two possible particle acceleration mechanisms: quasi-parallel and quasi-perpendicular. The comparison of synthetic maps of the Stokes parameter Q maps with observations proves to be a valuable tool to discern unambiguously which mechanism is taking place in the remnant of SN 1006, giving strong support to the quasi-parallel model.

Key words: MHD – radiation mechanisms: general – methods: numerical – supernovae: individual: SN 1006 – ISM: supernova remnants.

1 INTRODUCTION

Recently, the study of bilateral (also known as barrel-like) supernova remnants (SNRs) has gained great interest since they have proven to be a useful tool when studying the configuration of the interstellar magnetic field (ISMF) on scales of a few pc. As their name suggests, these type of SNRs display two characteristic bright and opposite arcs. The morphology of this type of remnants has been explained with an ISMF, which is involved in the acceleration mechanism of relativistic particles. However, there is still debate as to which is the most efficient acceleration mechanism in these objects. One interpretation is the equatorial belt model, in which the orientation of the ISMF is quasi-perpendicular to the shock front normal. The other interpretation is the polar cap model in which they are quasi-parallel.

The remnant of SN 1006 is the archetype of the bilateral SNR group. It has a diameter of 30 arcmin (or 20 pc at a distance of 2.2 kpc, Winkler, Gupta & Long 2003) and, in radio-continuum and X-ray images, exhibits an incomplete shell with two bright arcs perpendicular to the Galactic plane (Reynolds & Gilmore 1993; Reynoso, Hughes & Moffett 2013). SN 1006 is accepted to be the result of a Type Ia SN explosion (Stephenson & Green 2002). This remnant is located at a high Galactic latitude, and therefore thought to be evolving in an almost homogeneous interstellar medium (ISM). For this reason, the radio-continuum morphology of the remnant must be mostly affected by the characteristics of the surrounding ISMF.

Numerous theoretical and observational studies have been devoted to analyse which mechanism is responsible for the morphology of this remnant, giving rise to two opposing interpretations: either the quasi-perpendicular acceleration mechanism (e.g. Fulbright & Reynolds 1990; Petruk et al. 2009; Schneiter et al. 2010) or the quasi-parallel mechanism (e.g. Völk, Berezhko & Ksenofontov 2003; Rothenflug et al. 2004; Bocchino et al. 2011).

Most of these works apply criteria based only on the brightness distribution of the synchrotron emission. Accordingly, their conclusions are strongly dependent on the orientation of the ISMF respect to the line of sight (*los*), and cannot determine which particle acceleration mechanism is actually taking place. A recent observational polarization study seems to favour the idea that the bright arcs of SN 1006 can be explained by the polar cap model, implying an ISMF parallel to the Galactic plane (Reynoso et al. 2013).

This work is an effort to clarify which process or mechanism is more suitable to explain the synchrotron emission of the remnant of SN 1006. For this purpose, we carried out 3D magnetohydrodynamic (MHD) simulations employing the same scenario proposed in Schneiter et al. (2010). From the numerical results, we performed a polarization analysis of the Stokes parameters Q and U, as well as the polar-referenced angle, thus facilitating the direct comparison with observations.

The organization of this work is as follows: Section 2 presents the initial setup for the MHD simulations, Section 3 explains how the synthetic maps for the radio emission and Stokes Q and U

★ E-mail: mschneiter@gmail.com

parameters were calculated, Section 4 introduces the results obtained which are further discussed and summarized in Section 5.

2 THE NUMERICAL MODEL

2.1 Initial setup

The numerical simulations were carried out with the parallelized 3D MHD code MEZCAL (De Colle & Raga 2006; De Colle, Raga & Esquivel 2008; De Colle et al. 2012). This code solves the full set of ideal MHD equations in Cartesian geometry (x', y', z') with an adaptive mesh, and includes a cooling function to account for radiative losses (De Colle & Raga 2006). The computational domain is a cube of 24 pc per side and it is discretized on a six-level binary grid, with a maximum resolution of 2.3×10^{-2} pc. All the outer boundaries were set to an outflow condition (gradient free).

The SNR

The physical parameters of the SNR setup are the same as those presented in Schneiter et al. (2010), but to help the readability of this paper, we reproduce them below.

A supernovae explosion is initialized by the deposition of $E_o = 2.05 \times 10^{51}$ erg of energy in a radius of $R_0 = 0.65$ pc located at the centre of the computational domain. The energy is distributed such that 95 per cent of it is kinetic and the remaining 5 per cent is thermal.

The ejected mass was distributed in two parts: an inner homogeneous sphere of radius r_c containing 4/7ths of the total mass ($M_* = 1.4\ M_\odot$) with a density ρ_c, and an outer shell containing the remaining 3/7ths of the mass following a power law ($\rho \propto r^{-7}$) as in Jun & Norman (1996a). The velocity has a linear profile with r, which reaches a value of v_0 at $r = R_0$. The parameters ρ_c, r_c, and v_0 are functions of E_0, M_*, and R_0, and were computed using equations (1–3) of Jun & Norman (1996a).

The surrounding ISM

The surrounding ISM, where the SNR evolves, was simulated as an homogeneous plasma with temperature $T_0 = 10^4$ K and number density $n_0 = 5 \times 10^{-2}$ cm^{-3}. At a distance of ∼8pc in the x'-direction from the centre of the computational domain, the density was increased by a factor of 3 (Acero, Ballet & Decourchelle 2007). The SNR will collide with this 'wall', producing a bright Hα emission filament (Winkler et al. 2003), which has X-ray and radio counterparts (Acero et al. 2007; Schneiter et al. 2010).

In order to simulate the synchroton emission of SN 1006, based on the results of Schneiter et al. (2010), we have considered two configurations for the magnetic field $\boldsymbol{B}$ depending on which of the particle acceleration processes is assumed. For the quasi-perpendicular case, $\boldsymbol{B}$ is along the x'-direction, and it is along the y'-direction for the quasi-parallel case (the bright arcs are in the y'-direction). In both cases, we have considered a mean magnetic field magnitude of 2μG, while only for the quasi-parallel case an additional $\nabla \boldsymbol{B}$, increasing towards the $-x'$-direction, was included (which corresponds to model GRAD2 of Bocchino et al. 2011). Fig. 1 shows a scheme of the initial numerical setup employed in our simulations.

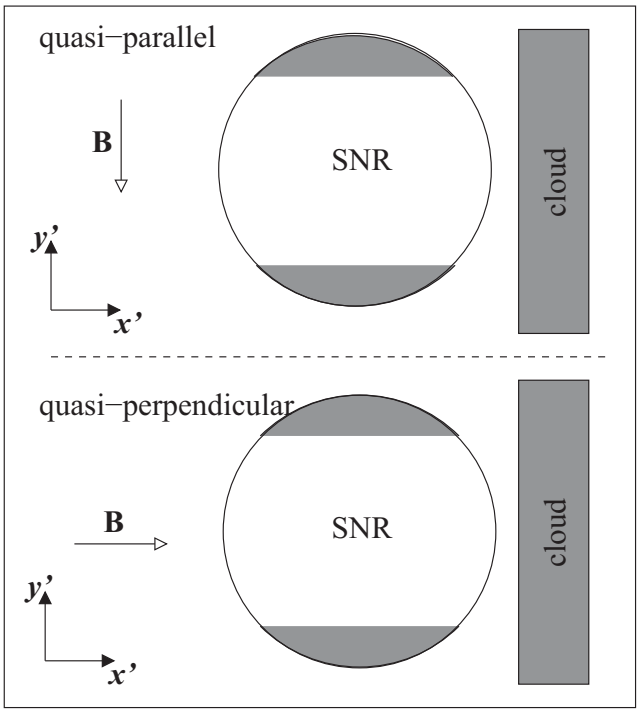

Figure 1. Scheme of the numerical setup employed in our simulations for the quasi-parallel (top panel) and the quasi-perpendicular case (bottom panel). In all the models, a dense cloud was placed to the right.

3 SYNTHETIC TOTAL AND POLARIZED RADIO EMISSION MAPS

3.1 Synchrotron emission maps

The synchrotron emission is obtained as (Ginzburg & Syrovatskii 1965)

$$i(\nu) \propto K B_\perp^{\alpha+1} \nu^{-\alpha}, \quad (1)$$

where ν is the observed frequency, $B_\perp$ is the component of the magnetic field perpendicular to the *los*, and α is the spectral index which was set to 0.6 for this object. The coefficient $K \propto \epsilon\ v_s^{-b}$ includes the dependence from the obliquity and the shock velocity v_s (Orlando et al. 2007), where ϵ is either proportional to $\sin^2\Theta_{Bs}$ for the quasi-perpendicular case or $\cos^2\Theta_{Bs}$ for the quasi-parallel case. The angle Θ_{Bs} is the angle between the shock normal and the post-shock magnetic field (Fulbright & Reynolds 1990). As in Orlando et al. (2007), the exponent b was chosen to be -1.5, implying that stronger shocks are more efficient injecting particles.

3.2 Maps of the Stokes parameters

To calculate the Q and U synthetic maps, the following expressions for the Stokes parameters were employed (see Clarke, Burns & Norman 1989; Jun & Norman 1996b)

$$Q(\nu) = \int_{los} f_0 i(\nu) \cos[2\phi(s)]\, ds \quad (2)$$

$$U(\nu) = \int_{los} f_0 i(\nu) \sin[2\phi(s)]\, ds, \quad (3)$$

where s increases along the *los*, $\phi(s)$ is the position angle of the local magnetic field on the plane of the sky, and f_0 is the degree of linear polarization, which is function of the spectral index α:

$$f_0 = \frac{\alpha + 1}{\alpha + 5/3} \tag{4}$$

The linearly polarized intensity is given by

$$I_P(\nu) = \sqrt{Q(\nu)^2 + U(\nu)^2} \tag{5}$$

and the polarization angle was computed as follows:

$$\chi = \frac{1}{2}\tan^{-1}(U/Q). \tag{6}$$

3.3 Observations

In order to compare our simulations with SN 1006 as observed in radio wavelengths, we have made use of data obtained at 1.4 GHz with the Australia Telescope Compact Array and the Very Large Array, already published in Reynoso et al. (2013). These data contain information on the polarization of the emission, thus we constructed a map of the polarized intensity (Fig. 2 a) and another map with the Q parameter (Fig. 3 a). The observations and data reduction process are described in Reynoso et al. (2013). The images presented here are convolved with a beam of 15 arcsec. To remove spurious features beyond the limits of SN 1006, only pixels where the total intensity is above 75 mJy beam^{-1} are retained.

4 RESULTS

4.1 Synthetic polarization maps

Synthetic polarized intensity maps were constructed from our numerical simulation results, using equation (5). Fig. 2 displays a comparison of the observed polarized emission (panel a), and the synthetic maps for the quasi-parallel (or polar cap model, panel b) and quasi-perpendicular (or equatorial belt model, panel c) cases. Before integrating along the *los* the computational domain (the $x'y'z'$- system) was tilted 60° counterclockwise around the z-axis (the *los*), such that the north points upwards and the east to the left (the plane of the sky is the xy plane). In addition, both models were rotated 15° around the y-axis. The quasi-parallel model was further rotated 15° in the x-axis. Both synthetic maps exhibit two bright arcs in the NE and SW direction, resembling the observations. The magnetic field gradient along the x-direction introduced in the simulations produces a SW–NE asymmetry in the polar cap model, in agreement with Bocchino et al. (2011) and with observations (see Reynoso et al. 2013, and Fig. 2 in this paper). As expected, the equatorial belt model shows greater intensity due to a higher efficiency in diffusive shock acceleration (Jokipii 1987; Rothenflug et al. 2004; Cassam-Chenaï et al. 2008).

4.2 Stokes parameter Q

In order to compare the simulated maps of the Stokes parameter Q with the observational one, we had to take into account that the observation of radio polarization from the SNR actually gives the position angle of the electric field. Hence, we had to follow the inverse process to the observational one, that is, the magnetic field was rotated clockwise 90°, emulating the perpendicular electric field, and then we performed the inverse Faraday correction. To clarify, we have replaced the argument $\phi(s)$ in the trigonometric

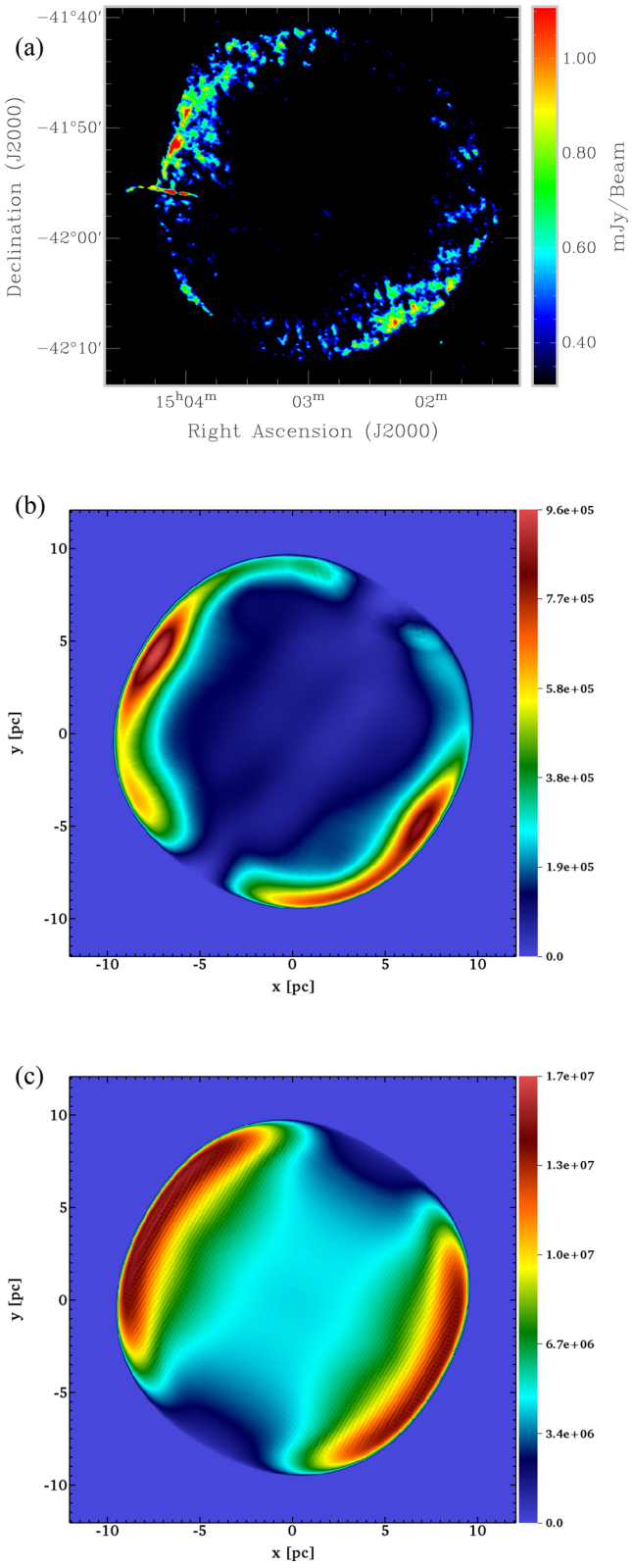

Figure 2. Synthetic maps of polarized intensity obtained for the quasi-parallel (panel b) and quasi-perpendicular (panel c) cases. The axes are in pc and the linear colour scale is in arbitrary units. These maps were rotated 60 deg with the purpose of comparing them to a radio image at 1.4 GHz (panel a), displayed in equatorial coordinates.

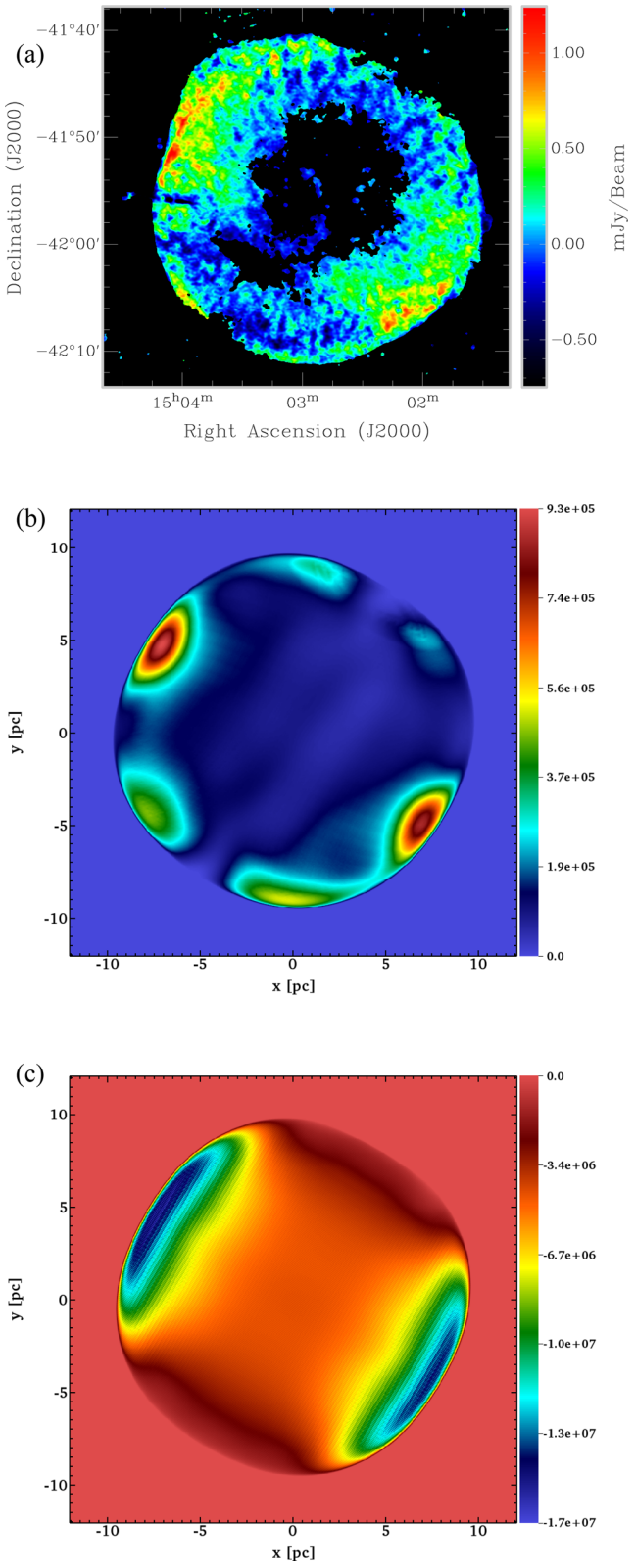

Figure 3. Comparison between the synthetic Stokes parameters Q for the quasi-parallel and the quasi-perpendicular cases (panels b and c, respectively) with observations (panel a).

functions of equations (2) and (3) by $\phi(s) - \pi/2 + \Delta\chi_F$, where $\Delta\chi_F$ is the Faraday rotation correction, given by

$$\Delta\chi_F = \frac{RM}{[\text{rad m}^{-2}]}\left(\frac{\lambda}{[\text{m}]}\right)^2 \quad (7)$$

being RM the rotation measure and λ the observed wavelength. For the case of the SN 1006, Reynoso et al. (2013) obtained an average RM of 12 rad m^{-2} from their polarization study at $\lambda = 0.21$ m. With these values, equation (7) gives a correction angle due to Faraday rotation of 0.52 rad or 30°.3.

Fig. 3 shows the resulting synthetic maps of the Q parameter (panels b and c for the quasi-parallel and the quasi-perpendicular cases, respectively), which were compared to the observed map (panel a).

As mentioned above, the question about which process of acceleration of relativistic particles is responsible for the synchrotron emission in SNRs (see Fulbright & Reynolds 1990; Völk et al. 2003; Rothenflug et al. 2004; Petruk et al. 2009; Schneiter et al. 2010; Bocchino et al. 2011) is an ongoing discussion in the literature. Our simulated polarized intensity maps are not conclusive on which of the two competing processes better explains the case of SN 1006. However, the maps of the Stokes parameter Q are quite different between the two models, thus removing the discrepancy. Hence, the Stokes parameters turn out to be an important tool to compare numerical models with observations and determine which of the acceleration processes is more suitable in each scenario.

4.3 Polar-referenced angles

Following Reynoso et al. (2013), we created maps of the angular difference for the position angle χ with respect to the local radial direction $\hat{r}$, i.e. we obtained maps with the distribution of the polar-referenced angle χ_r, which is given by

$$\chi_r = \cos^{-1}(\hat{r}.\hat{b}_\perp), \quad (8)$$

where $\hat{b}_\perp$ is the direction of the magnetic field on the plane of the sky. In this representation, $\chi_r = 0°$ and $\chi_r = \pm 90°$ correspond to the radial and tangential directions, respectively. These maps allow us to analyse two aspects of the magnetic field: the orientation of the post-shocked magnetic field and the orientation of the unshocked magnetic field of the ambient ISM. We expect the magnetic fields in young SNRs to be radially aligned due to the development of hydrostatic instabilities (Jun & Norman 1996b). So, the polar-referenced angle, χ_r, should have a value close to zero on the edge of the shell.

Fig. 4 shows maps of the distribution of χ_r, obtained for both quasi-parallel and quasi-perpendicular cases. These maps show a very small region on the SNR periphery with radial magnetic field orientation, and χ_r takes values that run from 0°(blue colour), to 90°(red colour). For both cases, the regions with $\chi_r \simeq 0$ are nearly aligned with the direction of the unperturbed magnetic field as imposed in each model. This 'radial' region is tilted clockwise ∼30° respect to the $\hat{y}$ or 'North' direction (see panel b of Fig. 4) for the quasi-perpendicular case, and ∼60° counterclockwise for the quasi-parallel case (see panel a of Fig. 4). The quasi-parallel model gives very good agreement (at large scales) with the observations (see figs 7a and b in Reynoso et al. 2013), suggesting that the direction of the ambient magnetic field proposed in this model must be representative of the actual orientation. We must note however, that the polar-referenced angles show some spread at small scales. This is most likely due to inhomogeneities of the magnetic field at such scales, which is not accounted for in our simulations.

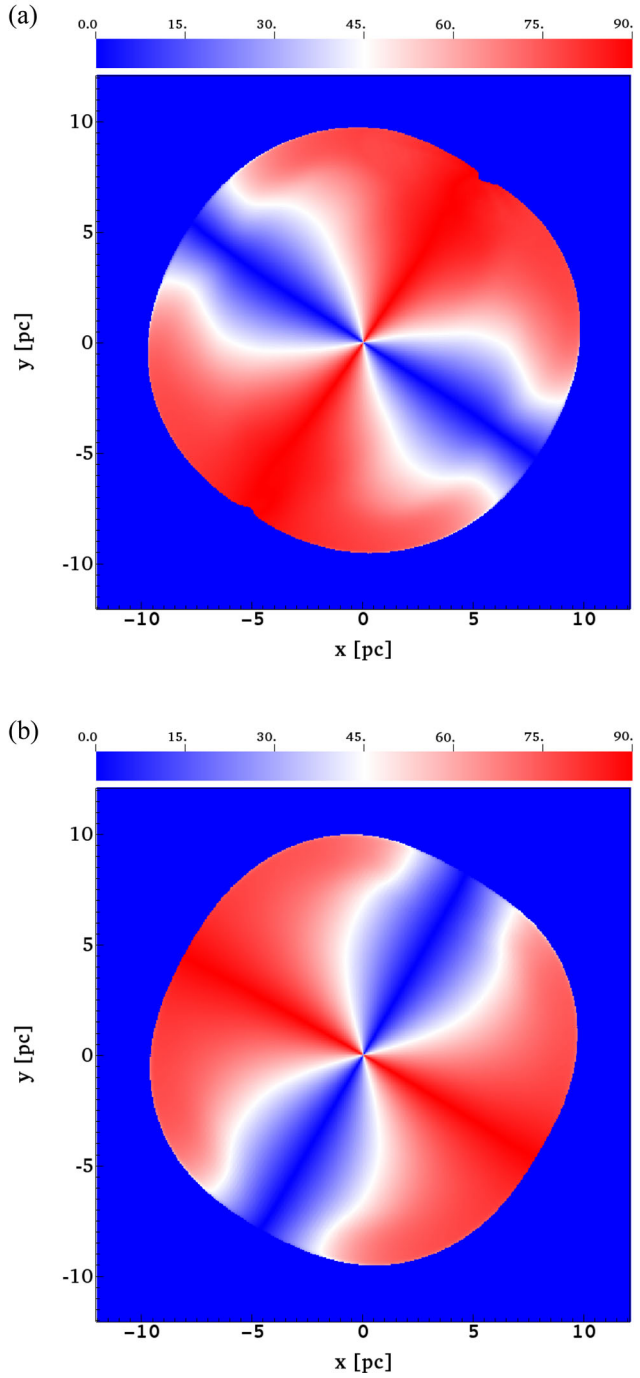

Figure 4. Synthetic polar-referenced angle maps obtained for the quasi-parallel (panel a) and quasi-perpendicular (panel b) cases. These maps were rotated 60 degrees with the purpose of comparing them to the observations. The axes are in pc and the linear colour scale is given in degrees.

5 DISCUSSION AND CONCLUSIONS

We have utilized 3D MHD models to simulate the polarized emission of SN 1006. The 3D simulations allow us to explore configurations that were impossible with the axisymmetric code used in Schneiter et al. (2010). In particular, it is possible to test different orientations of the magnetic field with respect to the plane of the sky and avoids some artefacts that arise when generating synthetic maps.

SN 1006 is a member of a population of 'barrel-like' or 'bilateral' SNRs. Previous studies (Reynolds & Gilmore 1993; Petruk et al. 2009; Schneiter et al. 2010; Bocchino et al. 2011; Reynoso et al. 2013) have shown that the emission geometry of bilateral SNRs is correlated with the orientation of the ambient ISMF. Different orientations of the magnetic field can be inferred depending upon which particle acceleration mechanism is assumed to be taking place at the SNR shock front, either the quasi-parallel or the quasi-perpendicular model.

As mentioned above, there is an ongoing debate as to which of these two particle acceleration mechanisms is responsible for the observed synchrotron emission in SNRs. While observational works seem to support the quasi-parallel model (polar cap scenario), theoretical studies are not conclusive. A probable reason for this discrepancy is that most of the theoretical works base their conclusions on criteria which only take into account the brightness distribution of the synchrotron emission.

In this work, we explore if a theoretical polarization study can be a useful tool to shed some light on this question. We synthesized maps of the polarized emission that include Stokes Q and U, and the distribution of the polar-referenced angle χ_r. In our analysis, we considered two scenarios: (1) an equatorial belt model where the bright rims of SN 1006 are formed from particle acceleration that occurs when the shock passes through ISMF that are perpendicular to the shock normal (quasi-perpendicular); (2) a polar cap model, where the bright rims are formed from acceleration that occurs when the shock passes through magnetic fields that are parallel to the shock normal (quasi-parallel).

The resulting polarized intensity maps alone are not sufficient to decide which mechanism is the adequate to explain the radio morphology of SN 1006 since both scenarios, quasi-parallel and quasi-perpendicular, yield similar results. On the contrary, the synthetic Q maps for the quasi-parallel and quasi-perpendicular cases differ much from each other. The quasi-perpendicular Q map displays regions with negative values resembling the bright rims observed in the polarized intensity maps. This result is in disagreement with the observations, which mainly display positive values (Fig. 3; see also Reynolds & Gilmore 1993). In addition, our simulated Q map for the quasi-parallel case coincides with observations in that the maxima are spatially coincident with the bright arcs of SN 1006, as obtained in our synthetic Q map for the quasi-parallel case. Finally, the synthetic polar-referenced angle map for the quasi-parallel model is in very good agreement with the results reported by Reynoso et al. (2013).

Our results agree with Bocchino et al. (2011) in that the ISM magnetic field must be parallel to the Galactic plane, tilted with respect to the *los*, and with a gradient that explains the assymetry in the emission between the arcs. The difference between their result and ours lies in the degree of inclination with respect to the *los*. For the parameter Q to be comparable to the observations, we employed an inclination of 75° with respect to the *los* (15° respect to the plane of the sky), which is somewhat larger than the best fit (38° ± 4°) reported in Bocchino et al. (2011).

We calculated the polar-referenced angle (χ_r) distribution and found good agreement with the observations of SN 1006 of Reynoso et al. (2013). The maps of observed χ_r show small-scale structure that is absent on our models due to the well-ordered field imposed. This technique might prove helpful for future studies that include the inhomogeneity of the media or of the magnetic field structure.

In summary, our polarization results provide a strong support to the quasi-parallel model, which is in agreement with previous observational (Reynoso et al. 2013) and theoretical works (Bocchino

et al. 2011). More importantly, the Stokes parameter Q proved to be a powerful tool to determine the particle acceleration mechanism that best explains the observed morphology and polarization seen in SN 1006. We note that in a previous 2D MHD numerical simulation, Schneiter et al. (2010) concluded that the quasi-perpendicular model was the most suitable to explain the observations. Our paper shows the importance of using 3D simulations, since limiting the analysis to what is possible with an axisymmetric setup led to an opposite result. Only a 3D model can account for a magnetic field that is tilted with respect to the *los* and can provide a realistic description of the particle acceleration and synchrotron emission of an SNR.

ACKNOWLEDGEMENTS

We thank the referee for his valuable comments which helped us to improve the original version of the manuscript. EMS and EMR are member of the Carrera del Investigador Científico, CONICET (Argentina). We acknowledge Enrique Palacios Boneta for maintaining the Linux server where our simulations were carried out. EMS, PFV, AE and FDC thank financial support from CONACyT (México) grants 167611 and 167625, CONACyT-CONICET grant CAR 190489 and DGAPA-PAPIIT (UNAM) IG100214, 101413, 103315 and IA101614. EMR is supported by CONICET grant PIP 112-201207-00226.

REFERENCES

Acero F., Ballet J., Decourchelle A., 2007, A&A, 475, 883
Bocchino F., Orlando S., Miceli M., Petruk O., 2011, A&A, 531, A129
Cassam-Chenaï G., Hughes J. P., Reynoso E. M., Badenes C., Moffett D., 2008, ApJ, 680, 1180
Clarke D. A., Burns J. O., Norman M. L., 1989, ApJ, 342, 700
De Colle F., Raga A. C., 2006, A&A, 449, 1061
De Colle F., Raga A. C., Esquivel A., 2008, ApJ., 689, 302
De Colle F., Granot J., López-Cámara D., Ramirez-Ruiz E., 2012, ApJ., 746, 122
Fulbright M. S., Reynolds S. P., 1990, ApJ, 357, 591
Ginzburg V. L., Syrovatskii S. I., 1965, ARA&A, 3, 297
Jokipii J. R., 1987, ApJ, 313, 842
Jun B.-I., Norman M. L., 1996a, ApJ, 465, 800
Jun B.-I., Norman M. L., 1996b, ApJ, 472, 245
Orlando S., Bocchino F., Reale F., Peres G., Petruk O., 2007, A&A, 470, 927
Petruk O. et al., 2009, MNRAS, 393, 1034
Reynolds S. P., Gilmore D. M., 1993, AJ, 106, 272
Reynoso E. M., Hughes J. P., Moffett D. A., 2013, AJ, 145, 104
Rothenflug R., Ballet J., Dubner G., Giacani E., Decourchelle A., Ferrando P., 2004, A&A, 425, 121
Schneiter E. M., Velázquez P. F., Reynoso E. M., de Colle F., 2010, MNRAS, 408, 430
Stephenson F. R., Green D. A., 2002, in Stephenson F. R., Green D. A., eds, International Series in Astronomy and Astrophysics Vol. 5, Historical supernovae and their remnants. Clarendon, Oxford
Völk H. J., Berezhko E. G., Ksenofontov L. T., 2003, A&A, 409, 563
Winkler P. F., Gupta G., Long K. S., 2003, ApJ, 585, 324

This paper has been typeset from a TEX/LATEX file prepared by the author.